

UC Irvine

UC Irvine Previously Published Works

Title

What is the "beta-induced Alfvén eigenmode?"

Permalink

<https://escholarship.org/uc/item/6kp9w2km>

Journal

Physics of Plasmas, 6(4)

ISSN

1070-664X

Authors

Heidbrink, WW
Ruskov, E
Carolipio, EM
[et al.](#)

Publication Date

1999-04-01

DOI

10.1063/1.873359

Copyright Information

This work is made available under the terms of a Creative Commons Attribution License, available at <https://creativecommons.org/licenses/by/4.0/>

Peer reviewed

What is the “beta-induced Alfvén eigenmode?”

W. W. Heidbrink,^{a)} E. Ruskov,^{b)} E. M. Carolipio, J. Fang, and M. A. van Zeeland^{c)}
University of California, Irvine, California 92697

R. A. James^{d)}
Lawrence Livermore National Laboratory, Livermore, California 94550

(Received 5 March 1998; accepted 14 December 1998)

An instability with a lower frequency than the toroidicity-induced Alfvén eigenmode was initially identified as a beta-induced Alfvén eigenmode (BAE). Instabilities with the characteristic spectral features of this “BAE” are observed in a wide variety of tokamak plasmas, including plasmas with negative magnetic shear. These modes are destabilized by circulating beam ions and they transport circulating beam ions from the plasma core. The frequency scalings of these “BAEs” are compared to theoretical predictions for Alfvén modes, kinetic ballooning modes, ion thermal velocity modes, and energetic particle modes. None of these simple theories match the data. © 1999 American Institute of Physics. [S1070-664X(99)00204-9]

I. INTRODUCTION

Intense, suprathermal fast-ion populations can drive instabilities. In tokamaks, the most extensively studied fast-ion driven instabilities¹ are the “fishbone” instability and the toroidicity-induced Alfvén eigenmode (TAE). In the DIII-D tokamak,² the frequency of the fishbone in the laboratory frame is typically 10–25 kHz, while the frequency of the TAE is generally 150–250 kHz.

During intense neutral beam injection into high-beta DIII-D plasmas, an instability of intermediate frequency was observed.³ This instability resembled the TAE, but the frequency was lower. The toroidal field B_T was scanned between 0.6 and 1.4 T. At each value of the toroidal field, injection of 5 MW of neutral beam power destabilized the TAE, but injection of 10 MW caused the frequency to drop to ~40% of the TAE frequency. The frequency of both instabilities scaled linearly with the toroidal field, as expected for Alfvén waves. The intermediate-frequency modes were only seen in plasmas with relatively large values of normalized beta, $\beta_N \equiv \beta_i a B_T / I_p \gtrsim 2.5$. (Here β_i is the toroidal beta in percent, a is the horizontal minor radius in meters, and I_p is the plasma current in MA.) Based primarily on these observations, the new instability was dubbed a beta-induced Alfvén eigenmode (BAE).

The characteristic experimental feature of this instability is a cluster of unstable peaks in the magnetics spectrum at a frequency intermediate between that of the fishbone and the TAE (Fig. 1). Each peak in the cluster corresponds to a different toroidal mode. In this paper, any instability with a cluster of intermediate frequency peaks is called an experimental “BAE.” A “BAE” is not necessarily an Alfvén eigenmode.

The “BAE” can expel large numbers of beam ions from the plasma. In one early experiment, internal vessel hardware was damaged in plasmas with both “BAE” and TAE activity.⁴ Under some conditions, “BAEs” caused the loss of over half of the beam power.

The “BAE” was first reported in low toroidal-field discharges in DIII-D.³ Subsequently, similar instabilities were observed in high-field DIII-D discharges⁵ and on the Tokamak Fusion Test Reactor (TFTR)^{6–8} and Joint European Torus.⁹ The TFTR “BAEs” may have been kinetic ballooning modes.⁶

Four possible theoretical identifications of the “BAE” have been proposed: an Alfvén eigenmode,¹⁰ a kinetic ballooning mode,¹¹ a mode that propagates at the ion thermal speed,¹² or an energetic particle mode.^{13–15}

This paper has two purposes: to document the experimental “BAE” with data from the DIII-D and TFTR tokamaks and to determine the correct theoretical identification of the instability. Although there are a number of points of agreement between the theoretical models and the experimental results, none of the theories match all of the data.

II. SURVEY OF THEORETICAL WORK

One of the proposed explanations for the “BAE” is that it is an Alfvén eigenmode. In cylindrical geometry in the ideal magnetohydrodynamic (MHD) model, the spectrum of shear Alfvén waves is continuous and the eigenmodes of the system are heavily damped. In a tokamak, however, gaps in the frequency spectrum are associated with departures from cylindrical symmetry:¹⁶ there is a toroidicity-induced gap,¹⁷ an ellipticity-induced gap,¹⁸ and a triangularity-induced gap. In addition to these gaps associated with coupling between two Alfvén waves of differing poloidal harmonics, there is a low-frequency gap caused by coupling between an Alfvén wave and a sound wave; geometrically, geodesic curvature and compressibility are responsible for the departure from cylindrical symmetry that creates the low-frequency gap.¹⁹ The size of this gap increases with increasing plasma beta.¹⁹

^{a)}Electronic mail: wwheidbr@uci.edu

^{b)}Present address: Princeton Plasma Physics Laboratory, Princeton, NJ 08543.

^{c)}Present address: DuraSwitch, Scottsdale, AZ 85251.

^{d)}Present address: LockheedMartin, Sunnyvale, CA 94089.

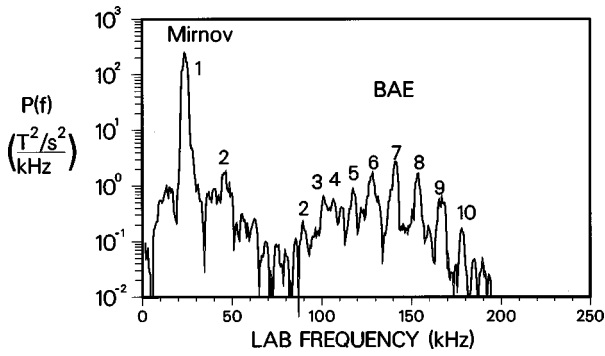


FIG. 1. An example of a “BAE cluster” in the cross-power spectrum of a pair of magnetic probes. The numbers beside the peaks indicate the toroidal mode number n of each mode. The “BAE cluster” is the set of peaks with $n=2-10$. The prominent peak near 20 kHz labeled “Mirnov” is produced by a mode that is essentially stationary in the plasma frame; the second ($n=2$), third, and fourth harmonics of this $n=1$ mode are also visible in the spectrum. Parameters: discharge 82989, 1021.5–1023.5 msec, $B_T=1.5$ T, $I_p=1.5$ MA, $\beta_N=2.4$, elongation $\kappa=2.0$, line-averaged electron density $\bar{n}_e=4.2 \times 10^{13}$ cm $^{-3}$, double-null divertor, and beam power $P_B=16$ MW.

Global eigenmodes with the dominant polarization of Alfvén eigenmodes exist in this “beta-induced” gap.¹⁰ For the beta-induced Alfvén mode, the predicted frequency scaling in the plasma frame is

$$f \propto f_{\text{TAE}} = B_T / (4\pi q R \sqrt{4\pi n_i m_i}). \quad (1)$$

For DIII-D, the mass density $n_i m_i$ is well approximated as $n_e m_d$, where m_d is the deuteron mass and n_e is the electron density. A kinetic theory of low-frequency Alfvén waves that included ion motion along the magnetic field found that, for subsonic modes, toroidal effects lead to an effective enhancement of the ion inertia and a large reduction in ion Landau damping.²⁰ The expected frequency of this subsonic beta-induced Alfvén mode is $f \lesssim f_{\text{TAE}}/2q$.

A second hypothesis is that the frequency of the “BAE” should depend on the ion thermal speed v_i . Numerical solutions of the equations of compressible resistive MHD found a global eigenmode at about half the frequency of the TAE.¹² Analytical arguments and numerical results indicated that the frequency of this eigenmode varies as the square root of the temperature, $\omega \propto \sqrt{T}$.¹² According to Ref. 20, a reduction in damping occurs when $f < \sqrt{r/R} f_{vi}/q$, where

$$f_{vi} \equiv \frac{\sqrt{2T_i/m_d}}{4\pi R}. \quad (2)$$

(Here r is the minor radius and T_i is the ion temperature.)

A third hypothesis is that “BAE” modes are actually kinetic ballooning modes. Analysis of the ballooning mode equations including energetic ion effects leads to the prediction of an unstable MHD gap mode with a frequency ω between $\omega_{*pi}/2$ and ω_{*pi} when the plasma is unstable to ideal ballooning modes.¹¹ Here

$$\omega_{*pi} = \frac{cT_i}{ZeB_T} k_\theta \nabla \ln p_i, \quad (3)$$

where c is the speed of light, T_i is the ion temperature, Ze is the ion charge, k_θ is the poloidal wave number, and p_i is the thermal ion pressure. Analysis⁶ of nine “BAEs” from TFTR

TABLE I. Theoretical “BAE” models.

Hypothesis	Nominal frequency scaling	Omitted dependence
Alfvén eigenmode	$v_A \propto B/\sqrt{n_e}$	β, q
Ion sound	$v_i \propto \sqrt{T_i}$	
Ballooning	$\omega_{*pi} \propto B^{-1} dp_i/dr$	η_i
Energetic particle	$v_{\text{circ}} \propto q^{-1}$	p

found that the measured frequencies scaled linearly with ω_{*pi} (correlation coefficient $r^2=0.6$). Also, the TFTR “BAEs” occurred in plasmas that were near the stability threshold for ideal ballooning modes.^{6-8,21} Subsequently, the theory was extended to include diamagnetic effects and plasma compressibility, with the conclusion that, in the most unstable regime, the kinetic ballooning modes are strongly coupled to Alfvénic modes due to the finite thermal ion temperature gradient $\eta_i \equiv (d \ln T_i/dr)/(d \ln n_i/dr)$.²² For comparisons with experiment, the predicted frequency $f = \omega_{*pi}/2\pi$ is evaluated using the approximation $k_\theta = nq/\rho a$, where n is the toroidal mode number and ρ is the normalized radial coordinate (the square root of the toroidal flux). The gradient of the ion pressure p_i is also evaluated in the horizontal midplane, $d \ln p_i/dr \approx d \ln p_i/d(ap)$.

The preceding three hypotheses identify the “BAE” with a weakly damped normal mode of the background plasma. For a plasma mode, the fast-ion population destabilizes the mode (alters ω_i) but has little effect on the mode frequency (ω_r). A fourth hypothesis is that the “BAE” is an energetic particle mode,¹³⁻¹⁵ that is, a wave branch that does not exist in the absence of an energetic particle population and whose real frequency ω_r is determined principally by the properties of the energetic ion population. When driven very strongly, the frequency of the predicted energetic particle modes depends solely on the circulation frequency of the energetic ions, $\omega = v_{\parallel}/qR$.¹⁵ However, for weaker drive, the numerical results indicate that the frequency also depends on the core pressure gradient.^{14,15} As the core plasma beta increases, there is a transition from a TAE to an energetic particle mode (EPM) to a kinetic ballooning mode.^{14,15} For a pure energetic particle mode, the laboratory frequency scales as

$$f_{\text{lab}} = v_{\parallel}/2\pi qR = f_{\text{EPM}}, \quad (4)$$

where v_{\parallel} is the velocity parallel to the magnetic field of the injected beam ions. In this paper, f_{EPM} is evaluated using the nominal angle of beam injection and the beam injection energy.

The expected parametric dependencies of the frequency for the four hypotheses are summarized in Table I. Important factors that are not included in the basic scaling relationships are also noted.

III. DETERMINATION OF THE EXPERIMENTAL FREQUENCY IN THE PLASMA FRAME

The predicted frequencies [Eqs. (1)–(4)] discussed in the previous section are local expressions that do not include the effect of plasma rotation. In reality, the measured frequencies

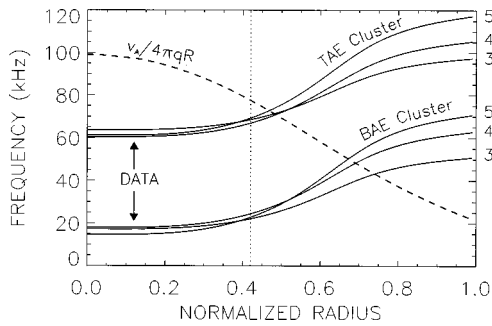


FIG. 2. Radial profiles of measured frequencies shifted to the plasma frame for two “clusters” of spectral peaks. Each mode is labeled by its toroidal mode number. The frequency in the plasma frame is $f = f_{\text{lab}} - n f_{\phi}$, where f_{ϕ} is obtained from a spline fit to the measured toroidal rotation of carbon. Also shown is the nominal frequency of the center of the TAE gap (dashed line). The various toroidal modes in a cluster have the same value of f at the “intersection radius” (dotted vertical line); in this case, the intersection radius is the same for the two clusters. The frequency of the upper cluster is consistent with a TAE, while the frequency of the lower cluster is that of a “BAE.” Parameters: discharge 71519, 2165–2167 msec, $B_p = 0.8$ T, $I_p = 0.6$ MA, poloidal beta $\beta_p = 1.3$, $\kappa = 1.6$, $\bar{n}_e = 5.1 \times 10^{13} \text{ cm}^{-3}$, inner-wall limiter, and $P_B = 10$ MW.

are affected by the structure of the radial eigenfunction and by the Doppler shift. This section explains how the experimental frequency measurements are related to local theoretical predictions.

Theoretically,²³ the frequency f in the frame where $\mathbf{E} = 0$ differs from the measured laboratory frequency f_{lab} due to the Doppler shift. Profiles of the toroidal plasma rotation f_{ϕ} are inferred from spectroscopic measurements²⁴ of the toroidal rotation of carbon which, except at the plasma edge, is nearly identical to the bulk plasma rotation.²⁵ Because all of the neutral beams in DIII-D inject parallel to the plasma current, the plasma rotates rapidly toroidally so

$$f \approx f_{\text{lab}} - n f_{\phi}, \tag{5}$$

where n is the toroidal mode number. Since the toroidal rotation f_{ϕ} is a function of position, the Doppler-corrected frequency in the plasma frame f is also a function of position (Fig. 2). The laboratory frequency f_{lab} and the toroidal mode number n are measured by a toroidal array of eight unevenly spaced magnetic probes;²⁶ the data are digitized at 500 kHz for all of the discharges in this study. Equation (5) states that the frequency in the ion frame f depends on the measured laboratory frequency f_{lab} , the measured toroidal mode number n , the measured rotation profile f_{ϕ} , and the radius of the mode. The first three quantities are known accurately for most DIII-D discharges. (Typical uncertainties are 0.5%, 0%, and 10% for f_{lab} , n , and f_{ϕ} , respectively.) In contrast, complete profiles of the radial eigenfunction are rarely available.

When “BAE” activity is observed by magnetic probes, the fluctuations are usually detected by some of the soft x-ray channels (Fig. 3), but adequate signal-to-noise for a full profile is rare. Good profile data are available for the case shown in Fig. 2, however. These measurements show that the “BAE” is most strongly excited in the plasma interior under these conditions. (The measured profile²⁷ for the TAE also peaks in the interior, although the structure differs

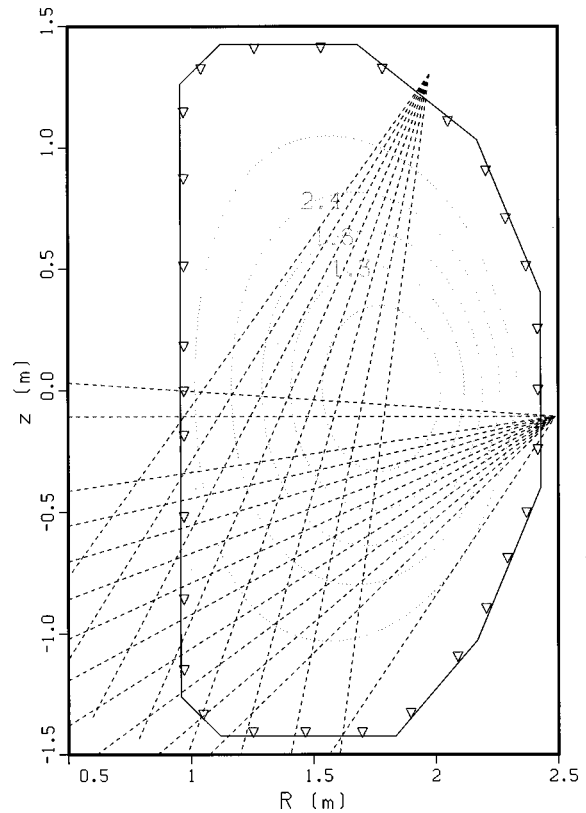


FIG. 3. Elevation of the DIII-D vacuum vessel showing the flux surfaces for discharge 71519 and the soft x-ray chordal views for the channels with valid fluctuation data. The q values of some of the flux surfaces are given.

from the “BAE.”) These data are also useful in disproving the hypothesis that the “BAE” is actually an edge TAE. The NOVA-K computer code calculated the eigenfunction of an $n = 3$ TAE in this discharge;²⁸ the eigenfunction peaks near $\rho \approx 0.9$ on the low-field side of the torus. Simulated chordal data based on this eigenfunction peak at larger radii than the measured profile (Fig. 4). The true eigenfunction of the “BAE” is large in the plasma core.

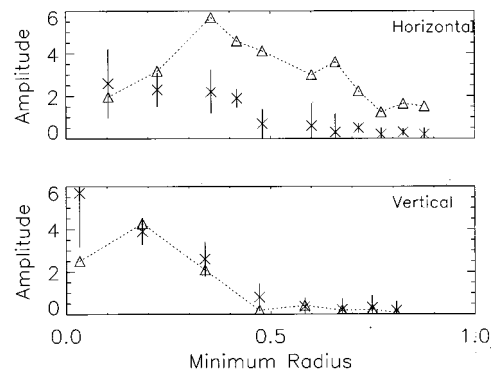


FIG. 4. Chord-integrated amplitude of the soft x-ray fluctuations for the $n = 3$ “BAE” at 51 kHz between 2165–2167 msec in discharge 71519. The data are plotted versus the minimum radius ρ of the soft x-ray chord (the distance of closest approach to the magnetic axis) for the horizontal camera (top) and for the vertical camera (bottom). The error bars are obtained from the incoherent background at 46 kHz. (Error bars obtained from the coherency are comparable.) Also shown (Δ) are the expected chord-integrated signals for the edge $n = 3$ TAE mode computed by NOVA-K.

Since the full radial eigenfunction is generally unavailable, ancillary assumptions are required to evaluate Eq. (5). In the construction of our database (Sec. IV), we have used two independent approaches. One approach is to evaluate f at fixed values of the minor radius ρ . The other approach, which is explained below, is to evaluate f at the “intersection radius” where the frequency of the various unstable toroidal modes are equal.

Apart from the lower frequency, the magnetics spectra for “BAEs” resemble the spectra for TAEs. In both cases, the principal “signature” of the instability is the appearance of a cluster of peaks in the magnetics spectrum (Fig. 1). A detailed study of TAE spectra in DIII-D concludes that the multiple toroidal modes have approximately the same frequency in the plasma frame and are excited at nearly identical radial locations in the plasma.²⁹ Figure 2 shows the Doppler-corrected frequency f as a function of radius for an unusual spectrum that contains a TAE cluster of peaks and a “BAE” cluster. (“BAE” and TAE clusters do not often coexist, but they do occasionally during the transition from one type of activity to the other.) The three different toroidal modes in the TAE cluster have the same frequency f near $\rho=0.42$. The value of f at this “intersection radius” is consistent with the theoretically expected TAE frequency. This behavior is typical for TAE spectra.²⁹ Surprisingly, the different toroidal modes in the “BAE” cluster also intersect near $\rho=0.42$! This suggests that the “BAE” frequency in the plasma frame is given by f at the “intersection radius,” as it is for the TAE.

In the following section, f is evaluated both at fixed radii and at the intersection radius.

IV. PARAMETRIC DEPENDENCIES

This section compares “BAE” data from different discharges with the four candidate theories discussed in Sec. II. In the first subsection, systematic scans and representative discharges are examined, while the latter subsections present results from DIII-D and TFTR databases.

A. Scans and representative discharges

A toroidal field scan between $B_T=0.6$ and 1.4 T in otherwise similar discharges is one of the best sets of data available for testing the theoretical predictions. (The plasma current was constant so the edge q and shear also varied as B_T changed; however, the central q only varied $\sim 20\%$ in these sawtooth discharges.) The results of this scan already appeared in the original paper on “BAE” modes.³ These data are compared with the four candidate theories of the “BAE” in Fig. 5. As previously reported, the frequency scales approximately linearly with the Alfvén speed, as expected for an Alfvén mode [Fig. 5(a)]. In contrast, the ion temperature only increases slightly with increasing B_T , so the prediction of the ion-thermal theory that $f \propto \sqrt{T_i}$ is in poor agreement with experiment [Fig. 5(b)]. The comparison with the kinetic ballooning mode theory is more subtle. The simplest prediction is that the frequency should scale with the pressure gradient, dp_i/dr . This simple prediction is inconsistent with the data [Fig. 5(c)]. On the other hand, the expected frequency

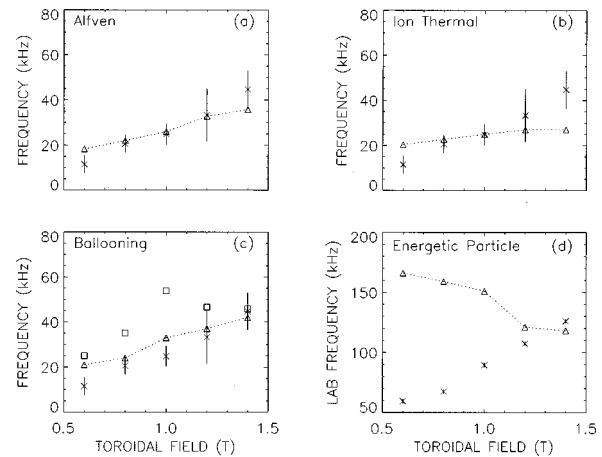


FIG. 5. Frequency versus toroidal field during a scan from 0.6–1.4 T in discharges like 71519; all frequencies are evaluated at the “intersection radius” (Sec. III). (a) Doppler-corrected frequency (\times) and $0.25f_{\text{TAE}}$ (Δ). (b) Doppler-corrected frequency (\times) and $\sqrt{T_i(0)}$ (Δ) (normalized at $B_T=1.0$). (c) Doppler-corrected frequency (\times) and $\omega_{*pi}/2\pi$ for two different assumptions about k_θ . In one case, $n=5$ is assumed (\square); in the other (Δ), the most unstable n for each datum is used in the evaluation of ω_{*pi} . (d) Laboratory frequency (\times) and f_{EPM} (Δ).

depends upon the poloidal wave number k_θ as well as on the pressure gradient [Eq. (3)]. During this scan, the most unstable toroidal mode n varied so that ω_{*pi} increased monotonically with B_T even though the pressure gradient did not [Fig. 5(c)]. Thus, the kinetic ballooning mode theory is consistent with experimental results for this scan. The prediction of the energetic particle mode theory [Eq. (4)], that the laboratory frequency should vary inversely with q , is inconsistent with the data for this scan [Fig. 5(d)].

The stability of “BAE” modes depends on the angle of beam injection. The DIII-D neutral beams inject at two orientations relative to the field: the so-called “left” beams inject more circulating beam ions (tangency radius $R_{\text{tan}} \approx 110$ cm) than the “right” beams ($R_{\text{tan}} \approx 76$ cm). A direct comparison of the angle of injection on “BAE” and TAE activity was already published in Fig. 8 of Ref. 30: in low-field (1.0 T), low-confinement, discharges with a conventional monotonically increasing q profile, “BAE” activity is driven more strongly by the left beams than by the right beams. A similar comparison for high-confinement, 2.0 T, reversed-shear discharges is shown in Fig. 6. Evidently, sub-Alfvénic circulating beam ions ($v_\parallel/v_A \approx 0.4$) also destabilize “BAE” activity more readily than trapped beam ions.

Another empirical observation is that “BAE” activity can be stabilized by lowering the beam injection energy. A reduction in energy from 75 to ~ 55 kV (even with a concomitant increase in the number of sources to maintain constant injected power) has suppressed the amplitude of “BAE” activity both in 1.0 T discharges and in 2.0 T discharges. In addition to reducing v_\parallel , lowering the voltage reduces the beam-ion density and flattens the beam-density gradient (by broadening the deposition profile), so it is not clear which physical effect is responsible for the improved stability.

The “BAE” activity has been observed in a wide vari-

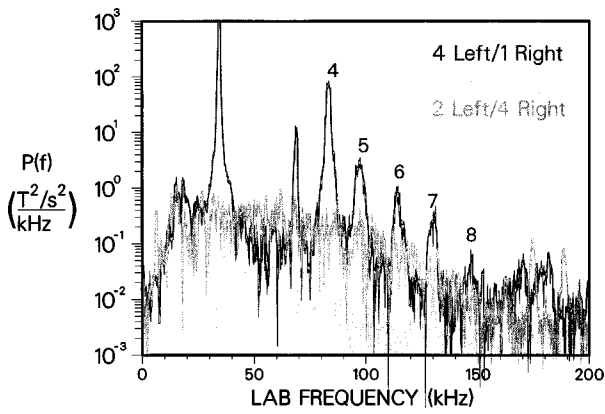


FIG. 6. Cross-power spectra for a pair of toroidally separated magnetic probes at 1735–1740 msec for three discharges with nearly identical plasma parameters but with different combinations of injected beams. The large “BAE” peaks were observed in the discharge with four left beams (black). The numbers beside the peaks indicate the toroidal mode number n of each mode in the “BAE” cluster. Parameters for the discharge with four left beams: discharge 87329, $B_T=2.1$ T, $I_p=1.8$ MA, $\beta_p=1.1$, $\kappa=2.0$, $\bar{n}_e=6.4 \times 10^{13}$ cm $^{-3}$, double-null divertor, and $P_B=11$ MW.

ety of plasma conditions. These include the original³ low-field DIII-D discharges with super-Alfvénic beam ions, supershots on TFTR,⁸ and the reversed-shear discharges shown in Fig. 6. The Alfvén gap structure for these three representative cases are shown in Fig. 4 of Ref. 3, Fig. 3 of Ref. 8, and Fig. 7 of this paper. Clearly, the modes can exist for a wide variety of gap structures. The plasma profiles for these three cases are compared in Fig. 8.^{31,32} Evidently, instability does not require a particular density, temperature, q , or rotation profile, nor does a threshold value of T_i/T_e or η_i seem essential. The MHD ballooning instability is also not necessary. Analysis of the profiles for the reversed-shear discharge shows that the measured pressure gradient is far from the infinite- n ballooning boundaries throughout the plasma core.

Another plasma condition with “BAE” activity is the high β_p regime in DIII-D.³³ Figure 9 shows the temporal evolution of a discharge with anomalously low beam-ion confinement. The discharge is formed by early beam injection into a low-current (0.6 MA), low-density plasma. The

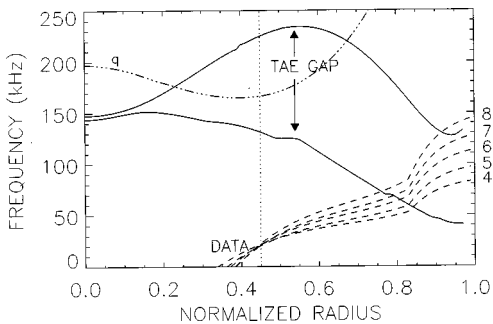


FIG. 7. Profiles of observed frequencies shifted to the plasma frame for the cluster of spectral peaks in discharge 87329. Each mode is labeled by its toroidal mode number n . Also shown is the envelope of the TAE gap as calculated by the CONT code (Ref. 19); the mode frequency at the intersection radius (dotted line) is in the beta-induced gap. The safety factor q (multiplied by 100) is also shown. [The MSE data were corrected for E_r effects (Ref. 40) in the equilibrium reconstruction.]

neutron emission, which is predominately produced by beam-plasma reactions in these conditions, indicates the development of a large beam-ion population around 800 msec. Concurrently, high-frequency magnetic activity is detected and persists throughout the period of high-power beam injection. Analysis of the magnetic spectra indicates that the instabilities are predominately “BAEs” that lie in the beta-induced gap in the Alfvén continuum of ideal MHD; there are also some weaker modes that fall in the TAE gap. During this phase of the discharge, the measured neutron emission is $\sim 40\%$ lower than the classically expected value. This anomaly in the beam pressure is corroborated by equilibrium reconstructions with EFIT,³⁴ which require $\sim 40\%$ reductions in the central beam-ion pressure (relative to the classical value) to achieve agreement with the location of the magnetic axis [as measured by electron cyclotron emission (ECE) and soft x-ray diagnostics]. The fast-ion contribution to the total stored energy W_{eq} must also be reduced to obtain a credible equilibrium. Additional evidence of anomalous beam-ion behavior is obtained from comparison of the equilibrium stored energy W_{eq} with the stored energy measured by a diamagnetic loop, W_{dia} . The plasma anisotropy $\Delta W_{\parallel} = 2(W_{eq} - W_{dia})$ is reduced during the “BAE” activity, presumably because the “BAEs” interact strongly with circulating beam ions. At 2550 msec the beam power is halved and the “BAE” activity ceases. Despite the reduction in beam power, the neutron emission and plasma stored energy barely change. This is consistent with the interpretation that $\sim 50\%$ of the beam power was expelled from the plasma during the high-power heating phase. Interestingly, ΔW_{\parallel} actually *increases* when the “BAE” activity ceases.

Active charge exchange data obtained during a toroidal field scan provide further evidence that “BAEs” degrade the confinement of circulating beam ions. In this experiment, 7 MW of the left neutral beams were injected into a low-density ($\bar{n}_e=4 \times 10^{13}$ cm $^{-3}$), 0.6 MA, double-null divertor plasma. The toroidal field was reduced from 2.1 to 1.0 T on successive discharges to alter the virulence of Alfvén activity. The amplitude of Alfvén activity steadily increased as the field was reduced, with the 2.1 T discharges being stable to Alfvén activity, the 1.7 T discharges containing occasional hints of instability, and the 1.0 and 1.4 T discharges evidencing clear, large amplitude clusters. Although the density barely changed during the scan, the neutron rate was a factor of 2 lower at 1.0 T than at 2.1 T. Since the neutron emission is predominately produced by beam-plasma reactions in these conditions, this reduction implies that $\sim 50\%$ of the beam power is lost [Fig. 10(a)]. Spatially resolved measurements of the 50 kV beam ions confirm that the reduction in neutron emission is caused by a loss of circulating beam ions from the plasma center. The data are obtained by a horizontally scanning neutral particle analyzer with a sightline that intersects two of the heating beams.³⁵ As the Alfvén activity increases in strength, the central density of beam ions decreases [Figs. 10(b) and 10(c)]. The reduction is not caused by classical effects, which account for $\leq 20\%$ of the reduction. [The density changed $< 10\%$ for discharges in the scan and, as shown in Fig. 10(b), changes in the classical thermalization time were small.] Concurrently with the reduction in

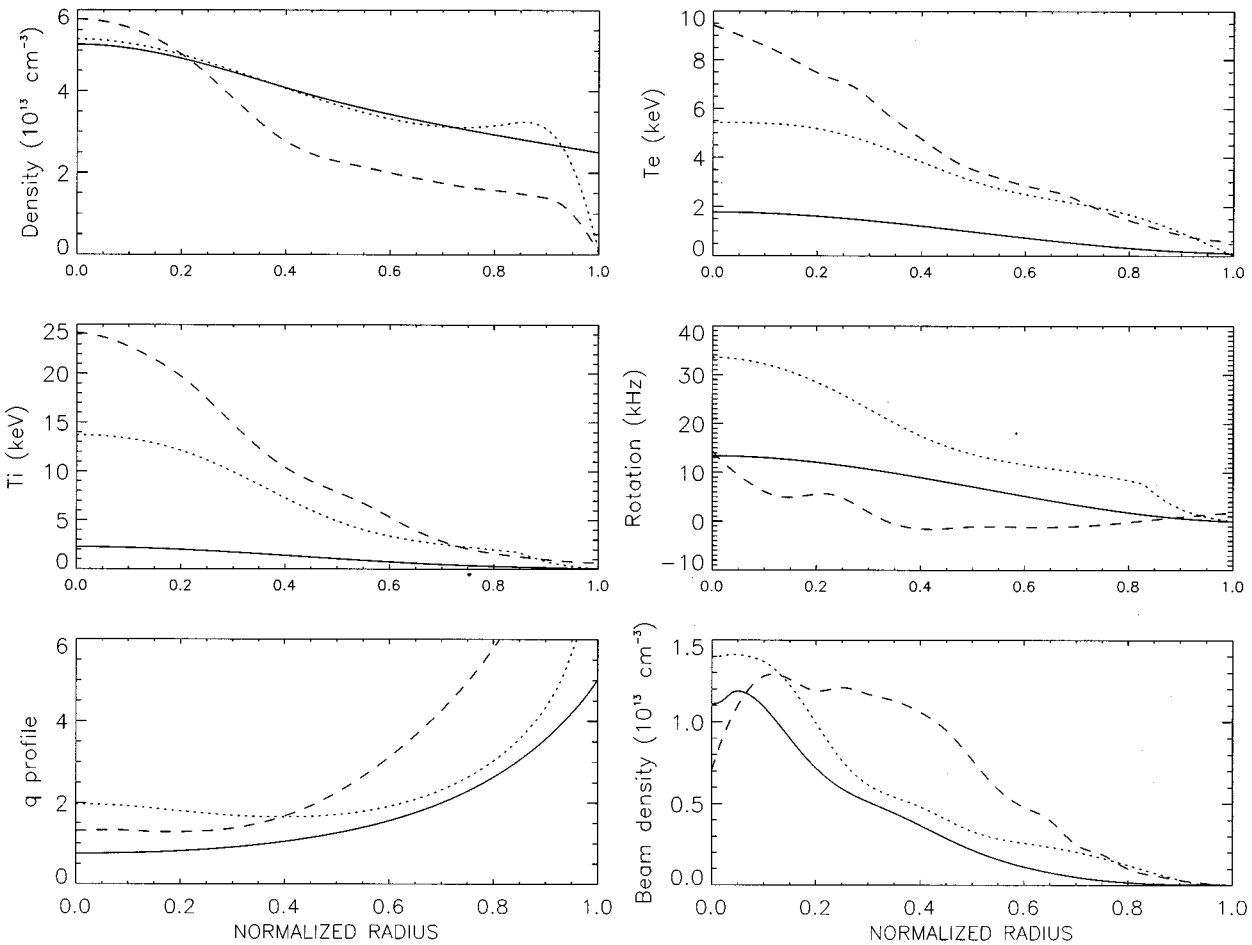


FIG. 8. Profiles of n_e , T_e , T_i , f_ϕ , q , and the classical beam density versus ρ for three different discharges: DIII-D low- B_T discharge 71519 (solid), DIII-D reversed-shear discharge 87329 (dotted), and TFTR supershot discharge 85863 (dashed). The first four profiles are from fits to the measured data, the q profile is from kinetic EFT reconstructions using MSE data, and the beam density is calculated by ONETWO³¹ (DIII-D) and by TRANSP³² (TFTR).

central beam-ion density, the passive charge-exchange signal produced by beam-ion collisions with edge neutrals increases [Fig. 10(b)]. The increase is probably caused by an increase in the number of beam ions at the edge, although the edge neutral density at the midplane may also increase (possibly due to bombardment of the walls by the escaping beam ions). The similarity between the observations for different pitch angles (Fig. 10) suggests that anomalous pitch-angle scattering is modest relative to radial transport.

B. DIII-D database

A representative sampling of over 200 DIII-D discharges from 1991–1996 were chosen for detailed analysis. For each discharge, dozens of magnetics spectra were evaluated and the discharge was classified as “stable” if no evidence of propagating modes below 250 kHz appeared in any of the spectra. Discharges were classified as “marginal” if only a few spectra showed evidence of clusters and if the amplitudes of the peaks were barely discernible above the noise. Discharges with many strong “BAE” clusters were categorized as unstable. Discharges with a single, constant frequency, propagating mode were classified as “solo” instabilities; although these modes are probably “BAEs,” they were excluded from the frequency study because the Doppler

shift at the intersection radius cannot be determined for a single peak (Sec. III). Modes with a frequency that “chirps” a factor of 2 in 1–2 msec occur rarely in DIII-D,³⁶ and only four examples of “chirping modes” appear in the database.

Profile analysis was performed for each of the selected discharges. First, the equilibrium was reconstructed by EFIT³⁴ using magnetics data and motional Stark effect (MSE) measurements of the internal field.³⁷ The electron density was measured by four CO₂ interferometers and by Thomson scattering,³⁸ the electron temperature by Thomson scattering and electron cyclotron emission,³⁹ and the ion temperature, toroidal rotation, and carbon density n_C were measured by charge-exchange recombination spectroscopy.²⁴ After mapping the measurements onto the equilibrium, spline fits to the profiles of n_e , T_e , T_i , f_ϕ , and n_C were performed. The fitted plasma data were then analyzed. The Alfvén gap structure was computed by the CONT code.¹⁹ The mode frequency in the plasma frame was obtained from the magnetics spectra and the profile of f_ϕ , as in Fig. 2. The predicted frequencies [Eqs. (1)–(4)] were computed. The ONETWO transport code³¹ calculated the classical beam density. All of these quantities at several radial locations were entered into a database.

The database was constructed before it was recognized that the radial electric field can have an appreciable effect

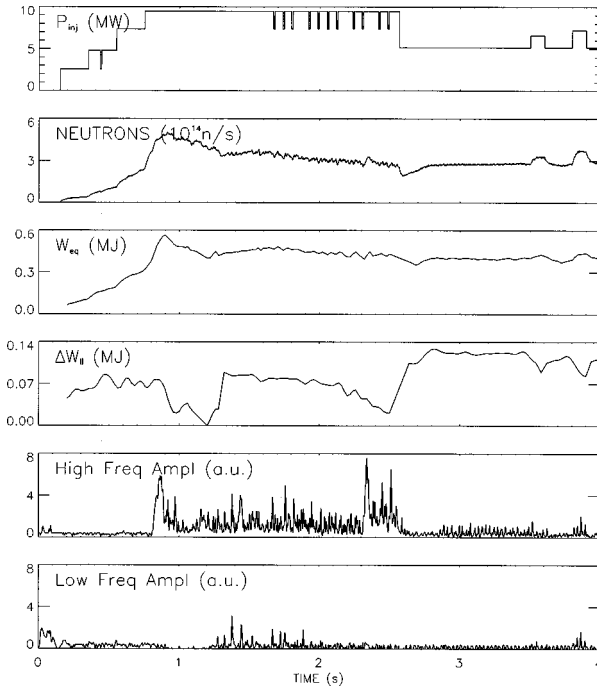


FIG. 9. Time evolution of the neutral beam power, the neutron rate, the equilibrium stored energy W_{eq} , the plasma anisotropy ΔW_{\parallel} , the amplitude of magnetic activity \dot{B} between 70–250 kHz, and the amplitude of magnetic activity \dot{B} below 25 kHz in a high- β_p discharge with anomalous beam–ion confinement. Parameters at 2160 msec: discharge 82941, $B_T=2.0$ T, $I_p=0.6$ MA, $\kappa=1.9$, $\bar{n}_e=2.7 \times 10^{13}$ cm $^{-3}$, $\beta_p=2.0$, and double-null divertor.

on the reconstructed q profile for high-performance discharges.⁴⁰ Also, in many cases, an automated fitting procedure was used to analyze the ion temperature and toroidal rotation from the charge–exchange recombination data. Thus, there are systematic errors in the database that are difficult to assess quantitatively. An example of the magnitude of these errors on the computed profiles is shown in Fig. 11. The errors in the profiles alter the frequencies in the database by $\lesssim 10\%$ (Table II). These uncertainties are too small to account for the poor correlation between theory and experiment that is discussed below.

For this database, the measured mode frequencies do not scale with any of the theoretical expressions. The Doppler-corrected frequency measurements were studied at several locations, including $\rho=0.25$, $\rho=0.50$, and the “intersection radius” (Sec. III), but the correlation with theoretical quantities is very weak at all radii. Figure 12 shows f as a function of the Alfvén speed; there is essentially no correlation. Any dependence of the frequency on the safety factor is weak (Fig. 12). The frequency of the BAE gap as calculated by CONT does not correlate with f either. The strongest frequency dependence in the database is the correlation of f with f_{TAE} at the intersection radius ($r^2=0.16$); f is essentially uncorrelated with f_{vi} and ω_{*pi} ($r^2=0.00$) at all radii. Also, the laboratory frequency f_{lab} does not correlate with f_{EPM} . The use of constraints based on the gap structure has no effect on these correlation coefficients.

In contrast to the data in the original paper on the “BAE,”³ for this larger set of data, the normalized Doppler-corrected frequency f/f_{TAE} does not correlate with β_N or

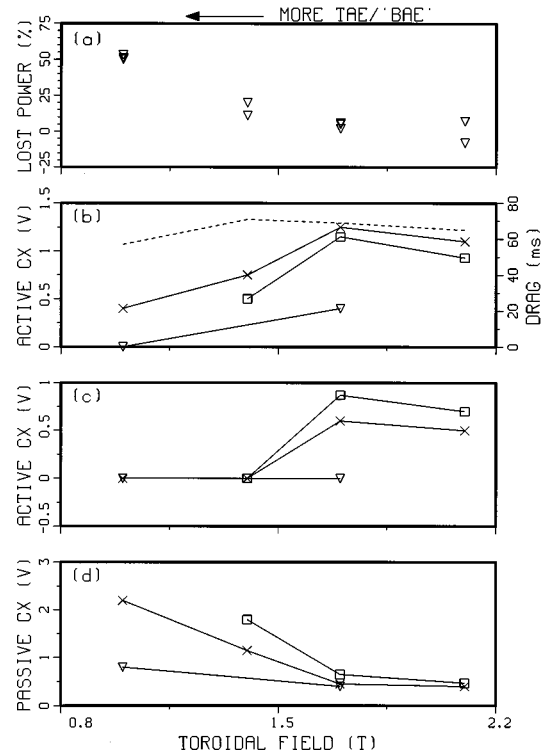


FIG. 10. (a) Fraction of the beam power that is lost from the plasma [inferred from the reduction in neutron emission (Ref. 4)] for the discharges in the 1994 toroidal field scan. The data are averaged between 1.6–2.4 sec. (b) Active charge exchange signal of 50 kV neutrals at 1.75 sec obtained by modulating the left 150° neutral beam for three different orientations of the neutral particle analyzer. The major radius and pitch angle $\cos^{-1}(v_{\phi}/v)$ of the measured neutrals: 1.55 m and 47° (∇), 1.83 m and 24° (\times), 2.04 m and 10° (\square). Also shown is the thermalization time ν_e^{-1} for 50 kV ions. (c) Active charge exchange signal at 1.75 sec obtained by modulating the right 150° neutral beam for three different analyzer orientations. The major radius and pitch angle of the measured neutrals: 1.40 m and 41° (∇), 1.78 m and 19° (\times), and 2.02 m and 7° (\square). (d) Passive (background) charge exchange signal at 1.75 s for three different analyzer orientations: tangency radius $R_{tan}=1.05$ (∇), 1.68 (\times), and 2.01 m (\square). Parameters for 81386 at 1.75 sec: injection energy $E_{inj}=75$ kV, $P_B=7.3$ MW, $B_T=1.7$ T, $I_p=0.6$ MA, $\beta_t=2.1\%$, $\kappa=2.0$, $n_e(0)=3.1 \times 10^{13}$ cm $^{-3}$, $T_e(0)=3.9$ kV, $T_i(0)=10.3$ kV, and double-null divertor.

β_p . (A minimum value of $\beta_N \geq 1.6$ or $\beta_p \geq 1$ is necessary for instability, however.)

The toroidal mode number of the most unstable mode does not correlate strongly with any of the parameters in the database, including the field (B_T, I_p, q), the shape (κ , triangularity δ), or the plasma parameters [$n_e(0), T_e(0), T_i(0), f_{\phi}(0), \beta_t, \beta_p$, the central beam beta β_b , $\eta = (d \ln T_i / dr) / (d \ln n_e / dr)$]. The most unstable toroidal mode number spans a similar range for the “BAE” as the TAE, although there is a slight tendency for instability to occur at lower values of n as the ion diamagnetic frequency increases (Fig. 13). (An inverse dependence of n on dp_i/dr is expected if the “BAE” is a hybrid Alfvén/kinetic ballooning mode with $\omega \sim \omega_{*pi} \sim \omega_{TAE}/2$.)

Identifying the free energy that drives the mode can provide insight into the nature of the instability. For both TAEs and “BAEs,” the beam parameters have the largest impact on stability. Instability is most likely if the beam ions are

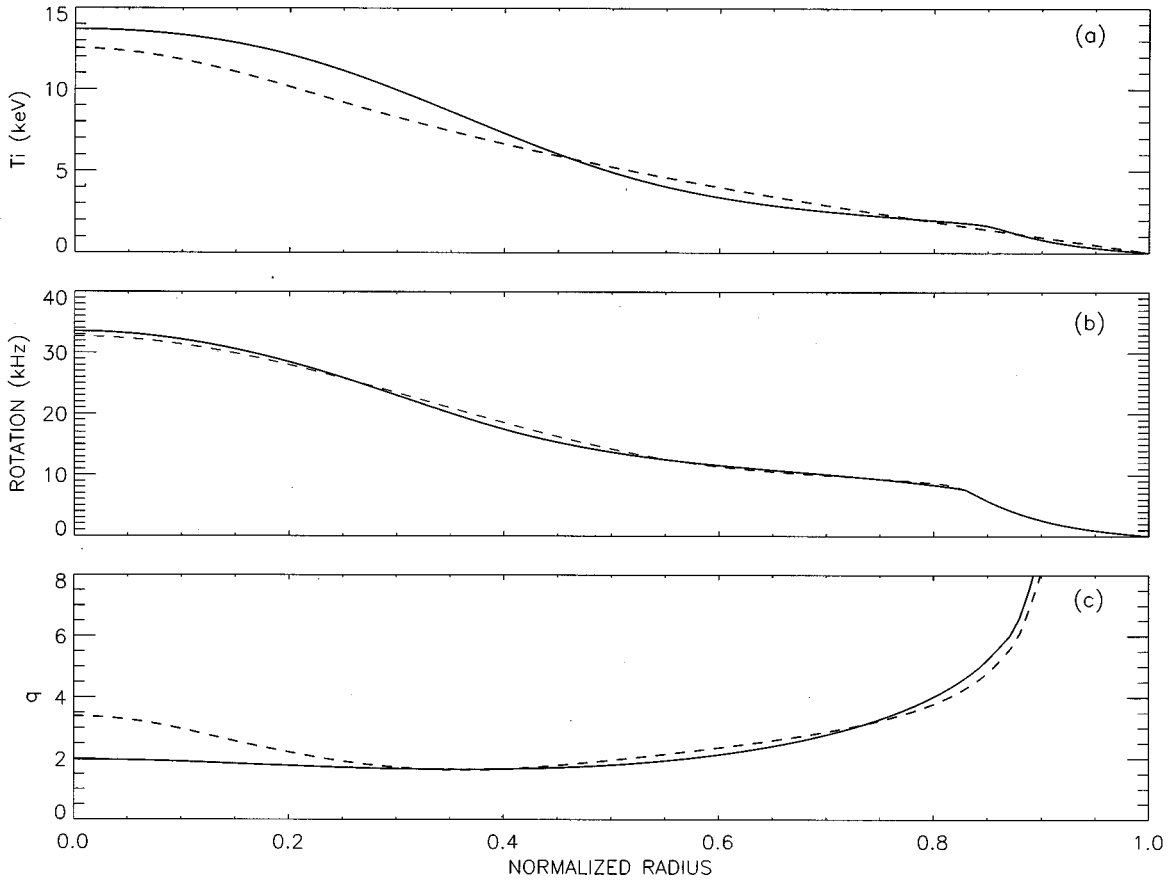


FIG. 11. The effect of different analysis techniques on the plasma profiles for discharge 87329. (a) Ion temperature profile from spline fits to charge-exchange recombination spectroscopy data analyzed by CERFIT (solid) and analyzed by an automated spectral fitting program (CERQUICK) (dashed). The difference in this case is larger than usual. (b) f_ϕ from spline fits to data analyzed by CERFIT (solid) and by CERQUICK (dashed). The difference in this case is smaller than usual. (c) q profile from an EFIT reconstruction that includes kinetic data, magnetics data, and MSE data that are corrected for E_r (solid) and from an EFIT reconstruction based on magnetics and uncorrected MSE data (dashed). The difference in this case is larger than usual because E_r is relatively large.

super-Alfvénic and if the gradient of the beam beta is large (Fig. 14). (The stability properties also correlate with β_b and with the stored beam energy, but the correlation is strongest with $d\beta_b/dr$.) The dependence on v_\parallel/v_A and on $d\beta_b/dr$ is similar for the “BAE” and the TAE. The stability properties do not depend systematically on any of the basic plasma parameters. There is also no correlation with ω_{*pi} , ω_{*pi}/ω_A , v_i , or v_i/v_A . In the theory of energetic particle modes, the beam-ion pressure gradient must exceed a certain threshold value;¹¹ the threshold condition $\alpha_f \approx -q^2(R/a)d\beta_b/dr \geq 0.7sv_\parallel/v_A$ is satisfied for all of the unstable modes in the database [here, $s=(r/q)dq/dr$ is the

magnetic shear], but the stability properties of the discharge do not depend upon the particular value of α_f .

In some discharges, only a single unstable toroidal mode is excited rather than a cluster of modes. To date, these “solo” instabilities with $f_{\text{lab}} > f_\phi(0)$ only occur in high performance discharges (Fig. 15) with high central electron temperature [$T_e(0) \geq 5$ kV], ion temperature [$T_i(0) \geq 12$ kV], and rotation frequency [$f_\phi(0) \geq 21$ kHz]. (Other parameters such as β_b , I_p , and β_p span similar ranges for clusters and solo peaks.) Perhaps the shear associated with strong rotation reduces the coupling between different toroidal modes.⁴¹

On occasion, “chirping” modes appear in the same frequency band as the “BAE.” These modes are distinguished by their rapid change in frequency, which drops by a factor of 2 in a single ~ 1 msec burst. (In contrast, the frequency of the “BAE” changes < 1 kHz in a single burst.) When chirping modes were first reported,³⁶ they had only been observed in six discharges; now, after examination of hundreds of additional discharges, five more discharges with chirping modes were found. The plasma regime for the recent observations is similar to the previously published conditions: the beam-ion population is large (volume-averaged classical beam beta $\geq 1\%$), the beam ions are sub-Alfvénic (v_\parallel/v_A

TABLE II. Effect of systematic errors in q , T_i , and f_ϕ on computed frequencies.

Frequency ^a	$\rho=0.25$	$\rho=0.50$	Intersection ρ
f [Eq. (5)]	-18/-14	29/26	25/21
f_{TAE} [Eq. (1)]	120/104	137/138	137/143
f_{vi} [Eq. (2)]	45/45	30/30	32/33
$\omega_{*pi}/2\pi$ [Eq. (3)]	164/246	62/67	78/79
f_{EPM} [Eq. (4)]	84/73	84/80	86/85

^aIn kHz for (best profiles)/(database profiles) in discharge 87329.

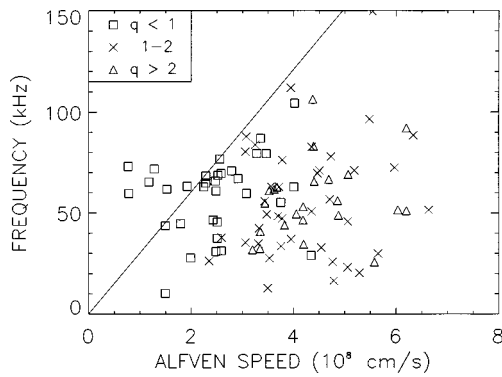


FIG. 12. Doppler-corrected frequency (at the intersection radius) versus the nominal Alfvén speed evaluated using the vacuum magnetic field and the line-averaged density for 96 DIII-D discharges with TAE or “BAE” clusters in the magnetics spectra. The symbols represent the minimum value of the safety factor.

<0.5), and the plasma is strongly rotating ($f_\phi \geq 20$ kHz). These are only necessary conditions for chirping, however; “BAEs” are more common than chirping modes even in plasmas that satisfy these conditions. Heidbrink³⁶ speculates that chirping modes occur when the conditions $f_{lab} \approx f_{EPM}$ and $f \approx 0$ are simultaneously satisfied; this can occur if the safety factor and rotation profiles are such that the product qf_ϕ is independent of radius. However, for the profiles in the database, there is no significant difference in qf_ϕ between the “BAE” plasmas and the chirping-mode plasmas (Fig. 16), so this hypothesis is discredited. It is not clear why “BAEs” appear more frequently than chirping modes.

The “BAEs” adversely affect beam-ion confinement. The database includes measurements of the neutron emission and two calculations of the expected emission. The ONETWO calculation³¹ uses a small-banana-width, steady-state beam distribution and the measured carbon density in a calculation that includes beam-beam reactions. A simple zero-dimensional code⁴² that neglects beam-beam reactions and assumes a constant deuterium concentration n_d/n_e also calculates the expected neutron emission. Both codes use recent fits to the $d(d,n)$ cross section.⁴³ If the beam ions behave

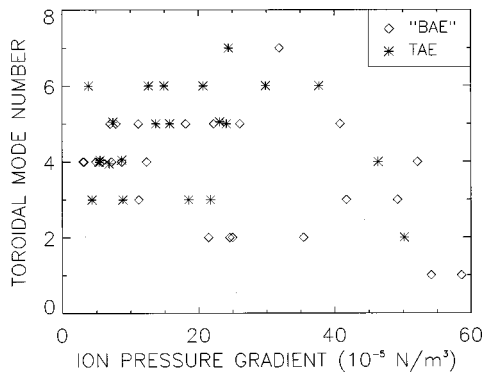


FIG. 13. Toroidal mode number n of the strongest mode versus maximum value of $-dp_i/dr$ for the clusters in the DIII-D database. The modes classified as TAEs have Doppler-corrected frequencies at the intersection radius that are >60% of the local value of f_{TAE} , while the modes classified as “BAEs” have $f < 0.6f_{TAE}$.

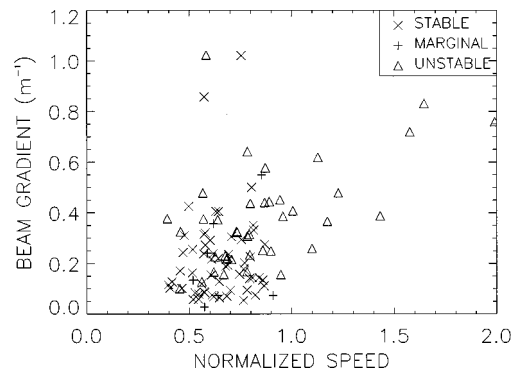


FIG. 14. Approximate gradient in the beam beta versus the nominal ratio of v_{\parallel} to v_A for the DIII-D database. Discharges without Alfvén instabilities are classified as stable, discharges with only a few small amplitude clusters are classified as marginal, and discharges with frequent strong clusters are “unstable.” The ordinate is the central beam beta calculated by ONETWO divided by the minimum value of the beam density scale length, $1/(d \ln \beta_b/dr)$. For the abscissa, v_{\parallel} is evaluated for full-energy beam ions injected by the left beams and v_A is evaluated using the vacuum toroidal field and the central electron density.

classically, the measured neutron rate approximately equals the calculated rate while, if the beam-ion confinement is anomalous, beam ions are lost before they can produce the expected number of fusion reactions. In stable plasmas, the ratio of the measured rate to the zero-dimensional code prediction is $S_{exp}/S_{cl} = 0.92 \pm 0.26$, in approximate agreement with classical expectations (Fig. 17). (Comparison with the ONETWO prediction is similar, but the correlation is weaker.) In contrast, the measured neutron emission is significantly smaller than the predicted emission (0.68 ± 0.30) in discharges with “BAEs” and TAEs. The magnitude of the reduction does not depend on the frequency of the mode (whether it is a “BAE” or a TAE). The anomaly is greatest for discharges with low neutron emission (many of which are low-field discharges with super-Alfvénic beam ions). However, even discharges with $S_{cl} > 10^{15}$ n/sec and “BAE” activity have suppressed neutron rates ($S_{exp}/S_{cl} = 0.78 \pm 0.30$), indicating that “BAEs” affect performance in high-performance plasmas with sub-Alfvénic beam ions.

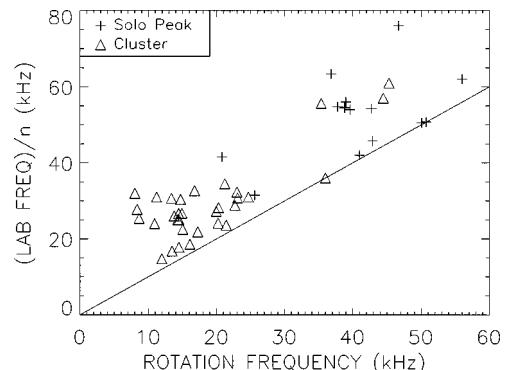


FIG. 15. Measured laboratory frequency divided by toroidal mode number versus central rotation frequency for isolated toroidal modes (+) and for “BAE” clusters (Δ). Only modes that propagate faster than the central rotation frequency [$f_{lab} > n f_\phi(0)$] are shown.

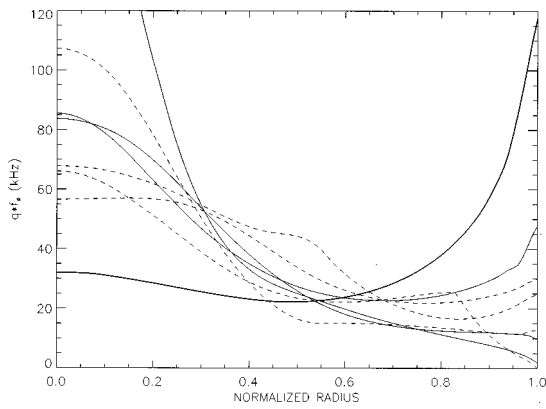


FIG. 16. Profiles of qf_ϕ as a function of ρ for chirping modes (solid lines) and for “BAEs” with $f_\phi(0) > 33$ kHz (dashed line). The heavy solid line is the profile in discharge 81382 that suggested the hypothesis (Ref. 36) that $f_{EPM} \approx n f_\phi$ for chirping modes.

C. TFTR database

A week of TFTR operation in April 1995 was devoted to “BAE” experiments in low-current (0.7–1.6 MA) supershots.⁸ The basic plasma parameters and magnetics data from this week were analyzed and entered into a database containing 119 “BAEs.”

In contradiction to the naive expectation for Alfvén modes, the laboratory frequency tends to decrease with increasing toroidal field (Fig. 18); however, for these TFTR plasmas with nearly balanced beam injection, the data needed to calculate $\mathbf{k} \cdot \mathbf{V}_E$ are unavailable, so the scaling of the Doppler-corrected frequency with v_A is uncertain. The correlation of laboratory frequency with v_A is similar to the correlation with B_T . As noted earlier,⁸ discharges heated with a combination of deuterium and tritium beams are similar to discharges heated by pure deuterium beams, which indicates that the weak alpha-particle population ($\beta_\alpha \leq 0.1\%$) does not have an appreciable effect on “BAE” stability under these conditions.

The laboratory frequency is weakly anticorrelated with the beam power ($r = -0.50$) and does not correlate (r^2

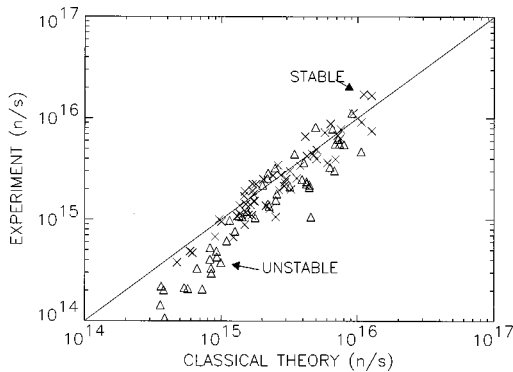


FIG. 17. Measured neutron rate versus classically expected rate for the discharges in the DIII-D database. Discharges with “BAE” or TAE clusters are represented by a Δ , while discharges without detectable clusters are represented by a \times . The line indicates perfect agreement. The classical prediction is from a zero-dimensional code (Ref. 42).

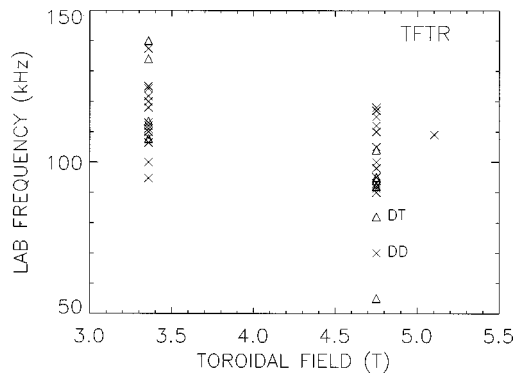


FIG. 18. Observed frequency of the strongest “BAE” mode versus toroidal field for the discharges in the TFTR database. Discharges fueled by both tritium and deuterium beams are indicated by a Δ .

< 0.1) with any other parameters in the database (n_e , β_p , stored energy W , I_p , and energy confinement time τ_E).

The toroidal mode number of the most unstable “BAE” tends to decrease with increasing toroidal field for these data (Fig. 19). The most unstable n does not correlate with any other parameters in the database.

V. TEMPORAL EVOLUTION

In this section, the temporal evolution of the frequency and stability properties of representative DIII-D discharges are presented, followed by a discussion of the expected evolution for each of the four theoretical models.

Figure 20 shows the temporal evolution of the frequency in a 1.0 T discharge. At 1500 msec, approximately 10 MW of left beams were injected; the first detectable instabilities occur ~ 35 msec later. The modes occur in bursts. As the discharge evolves, both the laboratory frequency and the Doppler-corrected frequency decrease. Comparison with the nominal TAE frequency indicates that the frequency of the first burst is close to the TAE frequency but the frequency steadily drops into the “BAE” range as the discharge evolves.

The first detectable instability does not appear until the neutron emission has risen to $\sim 60\%$ of its maximum value. The delay of ~ 35 msec is comparable to the central slowing-

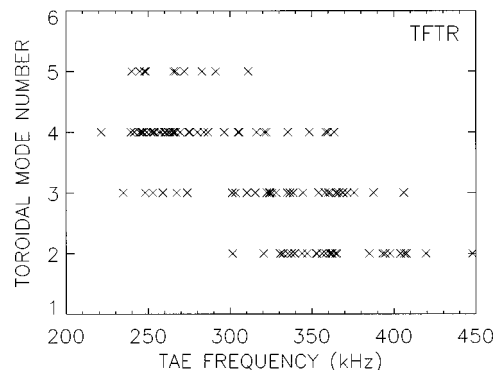


FIG. 19. Mode number n of the strongest mode versus f_{TAE} for the discharges in the TFTR database. The vacuum toroidal field, line-average electron density, and $q = 1.5$ were used to evaluate f_{TAE} .

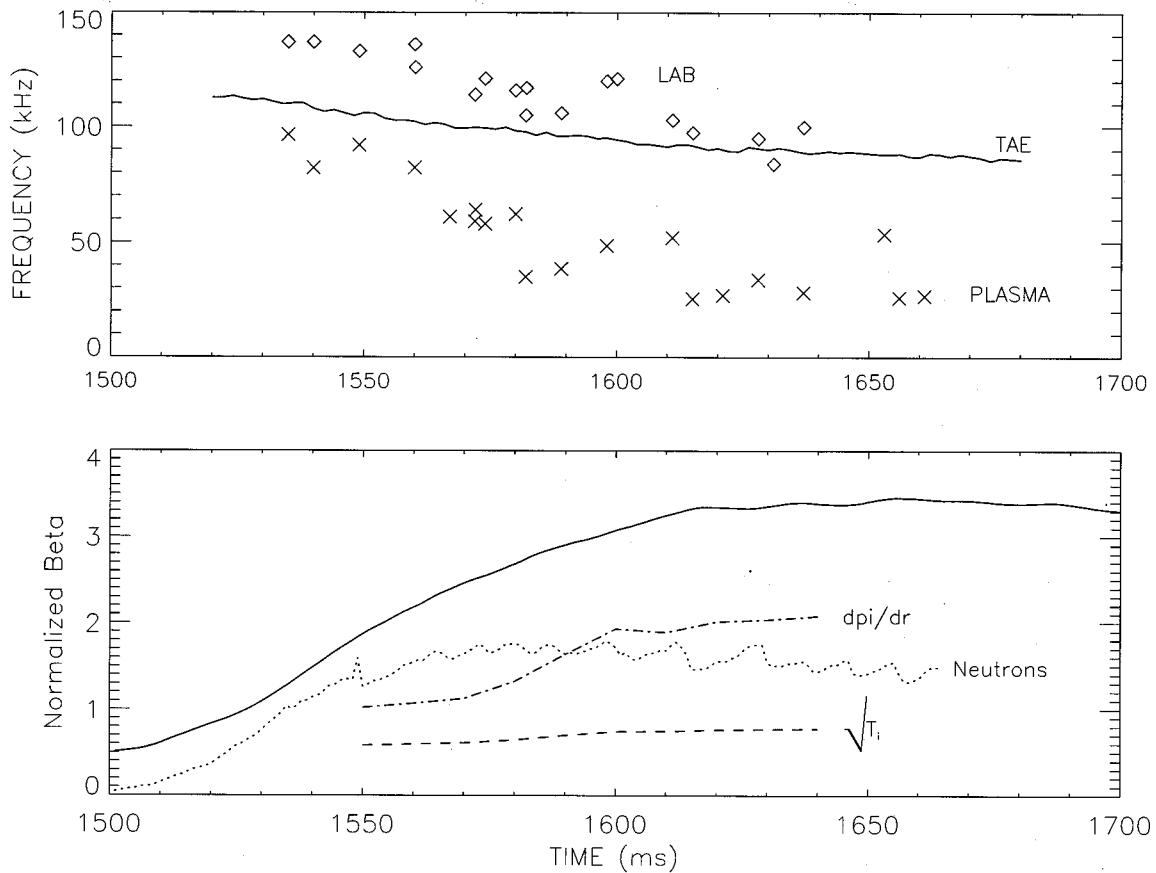


FIG. 20. (a) Time evolution of the observed frequency of the strongest mode in the cluster (\diamond), of the Doppler-corrected frequency at the intersection radius (\times), and of the nominal TAE frequency f_{TAE} (solid line) (evaluated using \bar{n}_e and $q=1.5$) for a DIII-D discharge in which 10 MW of left beams were injected beginning at 1500 msec. (b) Time evolution of the normalized beta β_N (solid), the neutron rate (dotted), the maximum value of the ion pressure gradient (dot-dash), and $\sqrt{T_i}(0)$ (dash). Parameters: discharge 71495, $B_T=1.0$ T, $I_p=0.6$ MA, $\kappa=1.6$, and inner-wall limiter.

down time for 75 kV beam ions, but is considerably shorter than the pitch-angle scattering time of ~ 240 msec. (Electron drag predominates.) In these conditions, calculations indicate that beam-plasma reactions constitute the dominant component of the neutron emission, so the neutron rate depends approximately linearly on the number of confined energetic beam ions. Thus, instability does not occur until β_b is appreciable. Since large velocity-space gradients probably occur 10–20 msec following the onset of beam injection, the 35 msec delay suggests that the TAE instability is driven primarily by spatial gradients in the beam pressure⁴⁴ rather than by anisotropy in velocity space.⁴⁵

The “transition” from TAE to “BAE” activity shows a wide variety of behaviors (Fig. 21). Sometimes the frequency gradually evolves with the plasma pressure (as in Fig. 20) but, in other cases, the frequency evolution does not correlate with the plasma energy. Comparison of the two discharges 71495 and 71496 is particularly interesting. These nominally identical discharges differ only in the angle of beam injection: 71495 was heated by left beams alone, while 71496 was heated by right beams only. As reported previously (Fig. 8 of Ref. 30), the amplitude of “BAE” activity is much larger for left beams than for right beams. In contrast to 71495, in 71496 the first detectable instability is a “BAE” and the frequency gradually *increases* as the discharge

evolves. Examination of Fig. 21 indicates that the frequency evolution does not correlate closely with the evolution of β_N .

In discharge 71496, the first burst appears 44 msec after the onset of beam injection (as the neutron emission nears its maximum value), suggesting that, like the TAE, the “BAE” is driven by β_b or $d\beta_b/dr$.

Several discharges with transitions from TAE to “BAE” activity were analyzed in an attempt to determine what parameters were responsible for the transition. The basic idea underlying the analysis is that, because beam-ion losses cause saturation of the beam-ion pressure near the point of marginal stability,⁴⁶ only the most unstable beam-driven instability appears at any given time. This expectation is consistent with the observation that TAEs and “BAEs” usually only coexist at transitions from one type of activity to another (cf. Fig. 21). Accordingly, parameters that affect the TAE and “BAE” stability should evolve at a transition. Figure 22 shows the analysis for the most interesting case. In this discharge, a relatively sharp transition to “BAE” activity occurred when the beam power was increased from 5.0 to 7.5 MW at 1900 msec, then a transition back to TAE activity occurred at ~ 2165 msec (possibly triggered by evolution in the q profile associated with an influx of impurities). A clear

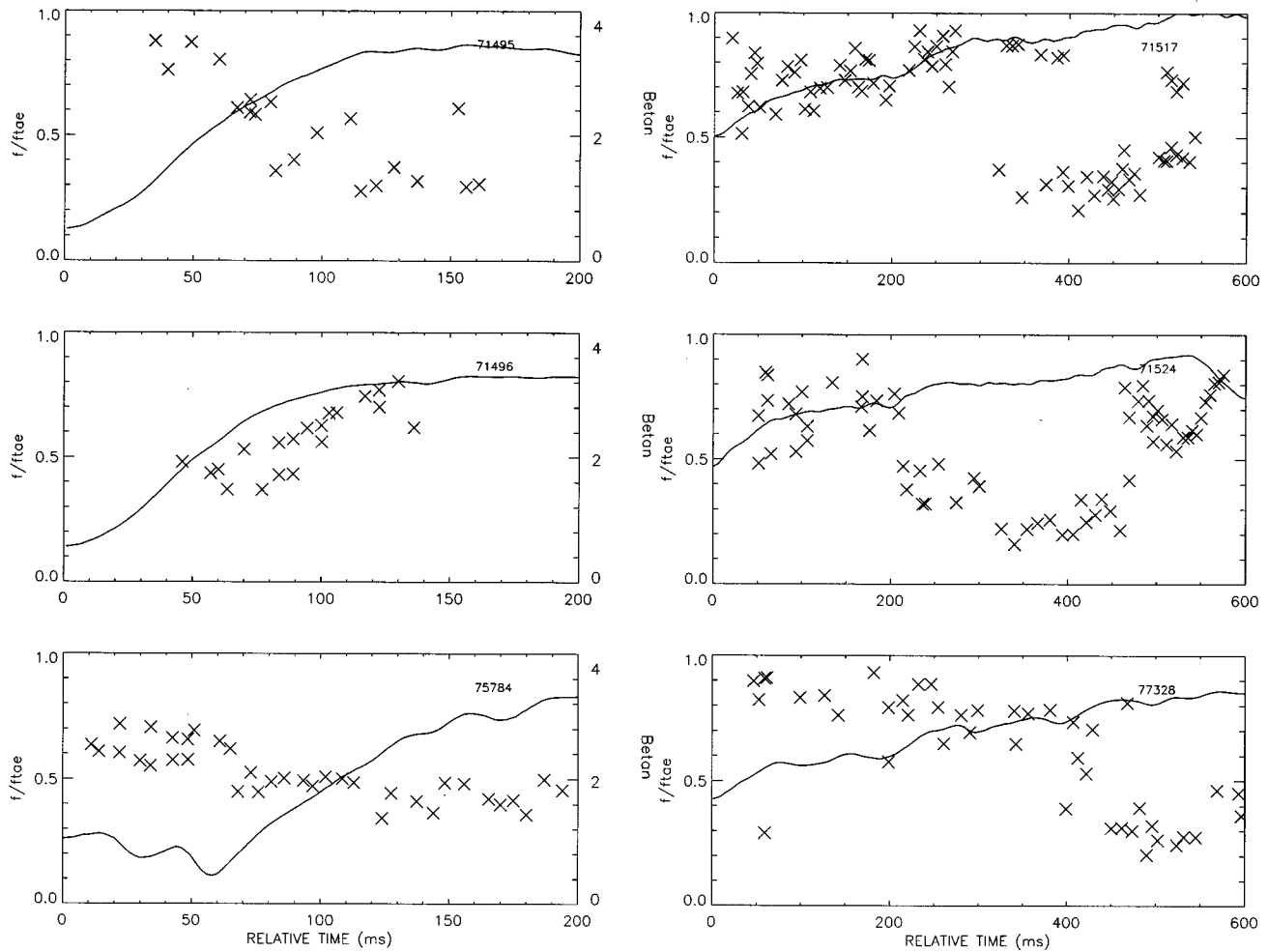


FIG. 21. Ratio of Doppler-corrected frequency at the intersection radius to nominal TAE frequency (\times) and evolution of β_N (solid line) for six different discharges. Discharge 71496 is identical to discharge 71495 except that right beams rather than left beams were injected. The parameters for 71517 resemble the parameters for 71519 and 71524 except that the toroidal field was $B_T=1.0$ T rather than 0.8 T. Parameters for 75784: $B_T=0.8$ T, $I_p=0.6$ MA, $\kappa=1.8$, $\bar{n}_e=2 \times 10^{13}$ cm $^{-3}$, inner-wall limiter, and $P_B=7$ MW; a minor disruption occurred ~ 40 msec earlier in the discharge. Parameters for 77328: $B_T=1.0$ T, $I_p=0.7$ MA, $\beta_p=1.4$, $\kappa=1.6$, $\bar{n}_e=4.3 \times 10^{13}$ cm $^{-3}$, inner-wall limiter, and $P_B=8$ MW.

“back transition” of this sort has only been observed in this discharge.

The data in Figs. 20–22 are difficult to reconcile with any of the proposed theoretical explanations for the “BAE.”

If the “BAE” is an Alfvén eigenmode, one expects a transition from eigenmodes that lie in the TAE gap to eigenmodes that fall in the beta-induced gap as the plasma parameters evolve. In some cases, the frequency seems to jump from one band to another but, in other cases, the evolution appears continuous (Fig. 21). Another difficulty is that transitions do not generally correlate with increases in β_N (Fig. 21) or with changes in the structure of the Alfvén continuum (Fig. 22). In earlier analysis of the stability of TAEs in DIII-D, a simple high- n calculation of radiative damping could account for the observed threshold in beam pressure,⁴⁷ however, changes in the calculated damping rate of the TAE do not account for the transitions either (Fig. 22).

In the simplest theory of the kinetic ballooning mode, the frequency depends linearly on ω_{*pi} ,⁴⁸ however, more refined theories predict a somewhat weaker dependence.¹¹ In contrast, in discharge 71495, f actually decreases with ω_{*pi}

(Fig. 20). Also, changes in the ideal ballooning properties of the plasma do not correlate with the transitions between TAE and “BAE” activity in discharge 71524 (Fig. 22).

The temporal evolution of the frequency in discharge 71495 is inconsistent with the expected evolution for an ion thermal mode (Fig. 20).

The hypothesis that the “BAE” is an energetic particle mode explains some of the observations. In discharge 71495 (Fig. 20), the laboratory frequency continues to drop for ~ 70 msec after the neutron emission has reached its maximum value. This evolution is inconsistent with the expected evolution of a pure energetic particle mode whose frequency depends only on $\langle v_{||} \rangle$. On the other hand, a parameter that evolves on the same time scale as the frequency is the plasma pressure (indicated by β_N) and this temporal evolution is reminiscent of the predicted dependence on core pressure for energetic particle modes.^{14,15} The gradual transitions that are sometimes observed (Fig. 21) are also consistent with identification of the “BAE” as an energetic particle mode. However, the frequency does not always evolve with

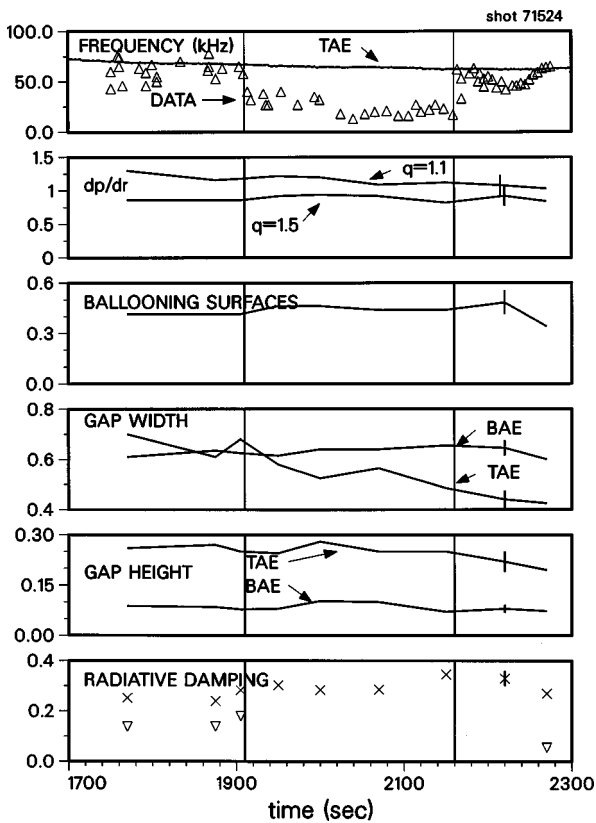


FIG. 22. Evolution of several parameters of theoretical interest in a discharge (71524) with two transitions between TAE and “BAE” activity (vertical lines). (a) Doppler-corrected frequency at the intersection radius and nominal TAE frequency. (b) Pressure gradients at the $q=1.1$ and $q=1.5$ surfaces (normalized to the first stability boundary for ideal ballooning modes). (c) Fraction of the plasma (in terms of the poloidal flux Ψ) in which ideal ballooning modes are unstable. (d) Radial extent of the TAE and BAE gaps, i.e., the horizontal width of the gap without intersecting the Alfvén continuum. (e) Vertical extent (in units of ω^2/ω_{A0}^2 , where $\omega_{A0} = v_A/qR$) of the TAE and BAE gaps at $q=1.5$. (f) Radiative damping ($-\gamma/\omega_r$) of the TAE calculated in the high- n limit at $q=1.5$ using the formalism of Mett *et al.* (Ref. 47) for the measured TAE frequency (∇) and for the theoretical (Ref. 47) eigenfrequency (\times). The vertical error bars at 2150 msec indicate the sensitivity of the calculated quantities to uncertainties in the experimental profiles.

changes in β_n (Fig. 21), which seems inconsistent with the model.

In summary, we have not found a simple, universally applicable explanation for the transition from TAE to “BAE” activity.

VI. DISCUSSION

Beam ions are expelled from the plasma by “BAEs.” Theoretically, there are two likely mechanisms for these losses. One is anomalous pitch-angle scattering across the passed/trapping boundary onto a loss orbit.⁴⁹ Another is resonant radial transport of circulating ions with little change in parallel velocity.⁵⁰ In an earlier DIII-D study, it was concluded that most lost beam ions spiral out radially with a step size of ~ 10 cm per toroidal transit, rather than suddenly jumping from a confined orbit to an unconfined orbit.⁴ The new data presented in this paper support this conclusion. The strong reduction in ΔW_{\parallel} (Fig. 9) indicate that passing ions

are most affected by “BAEs,” while the charge-exchange measurements (Fig. 10) imply strong radial transport with minimal pitch-angle scattering.

Of the models advanced to explain the “BAE” (Sec. II), the least successful of the four theories is that the “BAE” is a MHD mode whose frequency is governed by the thermal ion speed. Although the predicted mode frequencies are in the observed range, none of the frequency data scales with f_{vi} .

The idea that the “BAE” is a kinetic ballooning mode is consistent with some of the data. In previous work,⁶ the mode frequency measured in the plasma by a reflectometer was consistent with $\omega_{*pi}/2$ for nine TFTR discharges. In DIII-D, the frequency scaled with ω_{*pi} for a controlled toroidal field scan [Fig. 5(c)]. On the other hand, although the “BAE” frequency is usually in the expected range, the frequency does not scale with ω_{*pi} for an extended set of data from DIII-D. Also, the temporal evolution of the mode frequency is often opposite to that of ω_{*pi} (Fig. 20). Another difficulty is with the expectation¹¹ that the instability should occur near the MHD stability threshold. Although many discharges with “BAEs” are near the ballooning boundary,^{6–8,21} some (such as the discharge shown in Fig. 7) are well within the stable regime.

The hypothesis that the “BAE” is an Alfvén eigenmode also appears to have some merit but cannot explain all of the observations. A point of agreement is that the MHD code GATO¹⁰ computes centrally located modes with predominantly Alfvénic polarization that have frequencies that are consistent with the experimental observations for both the low-field DIII-D “BAEs”³ and for the TFTR supershots.⁸ Another successful prediction is that modes generally occur when the beta-induced gap in the Alfvén continuum is large. Moreover, the experimental “BAE” frequency usually (but not always) falls within this beta-induced gap. Another success is the scaling of the mode frequency with v_A for a toroidal field scan on DIII-D [Fig. 5(a)]. On the other hand, for a larger dataset from DIII-D, the frequency does not scale with v_A (Fig. 12) (although the correlation is higher with v_A than with any of the other predicted scalings). Also, for the TFTR data (Fig. 18), the laboratory frequency scales inversely with v_A , but the (unknown) Doppler-shift correction might modify this scaling. Another difficulty is with the time evolution of the frequency. Sometimes the frequency jumps suddenly from the TAE gap to the beta-induced gap but, in other cases, the frequency seems to evolve continuously (Fig. 21).

Another hypothesis with partial agreement is that the “BAE” is an energetic particle mode. The laboratory frequency is generally comparable to v_{\parallel}/qR , although the predicted parametric dependencies are not observed for the DIII-D toroidal field scan [Fig. 5(d)] or for the DIII-D or TFTR databases. In some cases, the frequency drops with core pressure (Fig. 20 and Fig. 2 of Ref. 3) as predicted qualitatively^{14,15} but, in other cases, the frequency is independent of β_N (Fig. 21).

It is possible that the “BAE” is a hybrid Alfvén eigenmode and kinetic ballooning mode, as suggested in Ref. 22. In the DIII-D toroidal field scan (Fig. 5), the toroidal mode

number of the most unstable mode varied with B_T in such a manner that the two conditions $f \propto f_{TAE}$ and $f \propto \omega_{*pi}$ were simultaneously satisfied. Perhaps this is the reason for the apparent dependence of n on dp_i/dr in DIII-D (Fig. 13) and for the dependence of n on v_A in TFTR (Fig. 19).

The parameters with the strongest effect on mode stability are the beam pressure and the angle of beam injection. Since all of the models assume the modes are destabilized by circulating beam ions, these observations are consistent with all four of the candidate explanations. The absence of any systematic dependence on other parameters (such as dp_i/dr for the kinetic ballooning mode or β_p for the Alfvén eigenmode) agrees best with the hypothesis that the “BAE” is an energetic particle mode.

VII. CONCLUSIONS

Propagating instabilities with frequencies below the TAE are often detected in DIII-D and TFTR plasmas with large circulating beam-ion populations. These “BAEs” often cause substantial reductions in the confinement of the circulating beam ions (Figs. 9, 10, and 17). The “BAEs” are dangerous instabilities that may be excited by alpha particles in a tokamak reactor.

The “BAEs” occur in a wide range of plasma conditions. Operationally, we have often attempted to stabilize “BAEs” in order to optimize plasma performance. Empirically, three fairly reliable techniques are to lower the beam voltage, lower the beam power, or switch to a more perpendicular angle of beam injection. All three of these “knobs” reduce the circulating beam-ion pressure.

There is no simple theoretical explanation for the experimental “BAE.” Our analysis is predicated on two assumptions. First, we have assumed that all instabilities with “BAE” signatures in the magnetics spectra are the same plasma mode, but this assumption may be erroneous. Perhaps different modes are excited under different conditions. Second, even if all “BAEs” are the same mode, our assumptions concerning the radial eigenfunction may be wrong. To compare with the local theoretical predictions, we either evaluated the frequencies at a fixed minor radius for every “BAE,” or we assumed that different toroidal modes rotate with the same rotation speed. If the actual radial eigenfunction has a complicated dependence on plasma conditions, the true frequency scaling was obscured by these assumptions. Alternatively, the failure of the data to match the predictions may originate in the theoretical approximations required to obtain simple analytical formulas. Portions of the data are consistent with the Alfvénic, kinetic-ballooning, and energetic-particle mode theories. It is quite possible that an accurate theoretical treatment of the “BAE” must include the beam-ion population^{14,15} as well as coupling between the Alfvénic and ballooning-mode branches.²²

ACKNOWLEDGMENTS

The assistance of R. Barron, K. Burrell, B. Rice, E. Strait, A. Turnbull, M. Wade, and the entire DIII-D team is gratefully acknowledged. We are also indebted to the TFTR team (particularly Z. Chang, E. Fredrickson, and J. Strachan)

for their assistance with the TFTR database. For Fig. 4, G. Huysmans kindly provided IDL routines for the soft x-ray comparison and G. Y. Fu calculated the TAE eigenfunction. M. Chu supplied working versions of the CONT code, and Y. R. Lin-Liu and R. Miller developed the code used to calculate ballooning stability. L. Chen, E. Lazarus, and T. Taylor provided helpful insights.

This work was principally supported by General Atomics subcontract SC-L134501 under U.S. Department of Energy contract DE-AC03-89ER51114, by DE-FG03-92ER54145 and W-7405-ENG-48, and by undergraduate research programs sponsored by the Department of Energy and the National Science Foundation.

¹W. W. Heidbrink and G. J. Sadler, Nucl. Fusion **34**, 535 (1994).

²J. L. Luxon and L. G. Davis, Fusion Technol. **8**, 441 (1985).

³W. W. Heidbrink, E. J. Strait, M. S. Chu, and M. S. Turnbull, Phys. Rev. Lett. **71**, 855 (1993).

⁴H. H. Duong, W. W. Heidbrink, E. J. Strait, T. W. Petrie, R. Lee, R. A. Moyer, and J. G. Watkins, Nucl. Fusion **33**, 749 (1993).

⁵W. W. Heidbrink, E. M. Carolipio, R. A. James, and E. J. Strait, Nucl. Fusion **35**, 1481 (1995).

⁶R. Nazikian, Z. Chang, E. D. Fredrickson, S. H. Batha, R. Bell, R. Budny, C. E. Bush, C. Z. Cheng, A. Janos, F. Levinton, J. Manickam, E. Mazzucato, H. K. Park, G. Rewoldt, S. Sabbagh, E. J. Synakowski, W. Tang, G. Taylor, and L. E. Zakharov, Phys. Plasmas **3**, 593 (1996).

⁷Z. Chang, R. V. Budny, L. Chen, D. Darrow, E. D. Fredrickson, A. Janos, D. Mansfield, E. Mazzucato, K. M. McGuire, R. Nazikian, G. Rewoldt, J. D. Strachan, W. M. Tang, G. Taylor, R. B. White, S. Zweben, and TFTR Group, Phys. Rev. Lett. **76**, 1071 (1996).

⁸W. W. Heidbrink, S. H. Batha, R. E. Bell, Z. Chang, D. S. Darrow, J. Fang, E. D. Fredrickson, R. A. James, F. M. Levinton, R. Nazikian, S. F. Paul, E. Ruskov, S. A. Sabbagh, R. A. Santoro, E. J. Strait, E. J. Synakowski, G. Taylor, A. D. Turnbull, K.-L. Wong, and S. J. Zweben, Nucl. Fusion **36**, 1725 (1996).

⁹A. Fasoli and S. Sharapov (private communication, 1998).

¹⁰A. D. Turnbull, E. J. Strait, W. W. Heidbrink, M. S. Chu, H. H. Duong, J. M. Greene, L. L. Lao, T. S. Taylor, and S. J. Thompson, Phys. Fluids B **5**, 2546 (1993).

¹¹S.-T. Tsai and L. Chen, Phys. Fluids B **5**, 3284 (1993).

¹²G. T. A. Huysmans, W. Kerner, D. Borba, H. A. Holties, and J. P. Goedbloed, Phys. Plasmas **2**, 1605 (1995).

¹³S. Briguglio, C. Kar, F. Romanelli, G. Vlad, and F. Zonca, Plasma Phys. Controlled Fusion **37**, A279 (1995).

¹⁴C. Z. Cheng, N. N. Gorelenkov, and C. T. Hsu, Nucl. Fusion **35**, 1639 (1995).

¹⁵R. A. Santoro and L. Chen, Phys. Plasmas **3**, 2349 (1996).

¹⁶J. P. Goedbloed, Phys. Fluids **18**, 1258 (1975).

¹⁷C. Z. Cheng and M. S. Chance, Phys. Fluids **29**, 3695 (1986).

¹⁸R. Betti and J. P. Freidberg, Phys. Fluids B **3**, 1865 (1991).

¹⁹M. S. Chu, J. M. Greene, L. L. Lao, A. D. Turnbull, and M. S. Chance, Phys. Fluids B **4**, 3713 (1992).

²⁰A. Bondeson and M. S. Chu, Phys. Plasmas **3**, 3013 (1996).

²¹Z. Chang, R. Nazikian, G.-Y. Fu, R. B. White, S. J. Zweben, E. D. Fredrickson, S. H. Batha, M. G. Bell, R. E. Bell, R. V. Budny, C. E. Bush, L. Chen, C. Z. Cheng, D. Darrow, B. LeBlanc, F. M. Levinton, R. P. Majeski, D. K. Mansfield, K. M. McGuire, H. K. Park, G. Rewoldt, E. J. Synakowski, W. M. Tang, G. Taylor, S. von Goeler, K. L. Wong, L. Zakharov, and the TFTR Group, Phys. Plasmas **4**, 1610 (1997).

²²F. Zonca, L. Chen, and R. A. Santoro, Plasma Phys. Controlled Fusion **38**, 2011 (1996).

²³T. S. Hahm and W. M. Tang, Phys. Plasmas **1**, 2099 (1994).

²⁴P. Gohil, K. H. Burrell, R. J. Groebner, and R. P. Seraydarian, Rev. Sci. Instrum. **61**, 2949 (1990).

²⁵J. Kim, K. H. Burrell, P. Gohil, R. J. Groebner, Y.-B. Kim, H. E. St. John, R. P. Seraydarian, and M. R. Wade, Phys. Rev. Lett. **72**, 2199 (1994).

²⁶E. J. Strait, Rev. Sci. Instrum. **67**, 2538 (1996).

²⁷E. M. Carolipio, W. W. Heidbrink, M. S. Chu, G. Y. Fu, A. Jaun, D. A. Spong, and R. White, Phys. Plasmas (to be submitted).

²⁸C. Z. Cheng, R. Budny, L. Chen, M. Chu, D. S. Darrow, E. D. Fredrick-

- son, G. Y. Fu, T. S. Hahm, C. T. Hsu, E. Mazzucato, H. E. Mynick, R. Nazikian, W. Park, N. Pomphrey, D. J. Sigmar, Y. Wu, R. B. White, and S. J. Zweben, "Energetic/alpha particle effects on mhd modes and transport," in *Plasma Physics and Controlled Nuclear Fusion Research 1994* (International Atomic Energy Agency, Vienna, 1995), Vol. 3, p. 373.
- ²⁹E. J. Strait, W. W. Heidbrink, and A. D. Turnbull, *Plasma Phys. Controlled Fusion* **36**, 1211 (1994).
- ³⁰E. J. Strait, W. W. Heidbrink, A. D. Turnbull, M. S. Chu, and H. H. Duong, *Nucl. Fusion* **33**, 1849 (1993).
- ³¹H. St. John, J. R. Ferron, L. Lao, T. Osborne, S. Thompson, and D. Wroblewski, in *20th EPS Conference on Controlled Fusion and Plasma Physics*, Lisbon, 1993 (European Physical Society, Petit-Lancy, 1993).
- ³²R. V. Budny, *Nucl. Fusion* **34**, 1247 (1994), and references therein.
- ³³P. A. Politzer, T. Casper, C. B. Forest, P. Gohil, W. W. Heidbrink, A. W. Hyatt, R. A. James, R. Jong, L. L. Lao, M. Makowski, W. Meyer, G. D. Porter, G. T. Sager, B. W. Stallard, H. St. John, S. J. Thompson, A. D. Turnbull, and D. Wroblewski, *Phys. Plasmas* **1**, 1545 (1994).
- ³⁴L. L. Lao, H. St. John, R. D. Stambaugh, A. G. Kellman, and W. P. Pfeiffer, *Nucl. Fusion* **25**, 1611 (1985).
- ³⁵E. M. Carolipio and W. W. Heidbrink, *Rev. Sci. Instrum.* **68**, 304 (1997).
- ³⁶W. W. Heidbrink, *Plasma Phys. Controlled Fusion* **37**, 937 (1995).
- ³⁷B. W. Rice, D. G. Nilson, and D. Wroblewski, *Rev. Sci. Instrum.* **66**, 373 (1995).
- ³⁸T. N. Carlstrom, G. L. Campbell, J. C. DeBoo, R. Evanko, J. Evans, C. M. Greenfield, J. Haskovec, C. L. Hsieh, E. McKee, R. T. Snider, R. Stockdale, P. K. Trost, and M. P. Thomas, *Rev. Sci. Instrum.* **63**, 4901 (1992).
- ³⁹M. E. Austin, R. F. Ellis, J. L. Doane, and R. A. James, *Rev. Sci. Instrum.* **68**, 480 (1997).
- ⁴⁰B. W. Rice, K. H. Burrell, and L. L. Lao, *Nucl. Fusion* **37**, 517 (1997).
- ⁴¹D. A. Spong, B. A. Carreras, and C. L. Hedrick, *Phys. Plasmas* **1**, 1503 (1994).
- ⁴²W. W. Heidbrink, P. L. Taylor, and J. A. Phillips, *Rev. Sci. Instrum.* **68**, 536 (1997).
- ⁴³H.-S. Bosch and G. M. Hale, *Nucl. Fusion* **32**, 611 (1992).
- ⁴⁴G. Y. Fu and J. W. van Dam, *Phys. Fluids B* **1**, 1949 (1989).
- ⁴⁵V. S. Belikov and O. A. Silivra, *Nucl. Fusion* **34**, 1522 (1994).
- ⁴⁶W. W. Heidbrink, H. H. Duong, J. Manson, E. Wilfrid, C. Oberman, and E. J. Strait, *Phys. Fluids B* **5**, 2176 (1993).
- ⁴⁷R. R. Mett, E. J. Strait, and S. M. Mahajan, *Phys. Plasmas* **1**, 3277 (1994).
- ⁴⁸H. Biglari and L. Chen, *Phys. Rev. Lett.* **67**, 3681 (1991).
- ⁴⁹D. J. Sigmar, C. T. Hsu, R. White, and C. Z. Cheng, *Phys. Fluids B* **4**, 1506 (1992).
- ⁵⁰R. B. White, R. J. Goldston, K. McGuire *et al.*, *Phys. Fluids* **26**, 2958 (1983).